Journal of Biomolecular Structure & Dynamics, ISSN 0739-1102
Volume 19, Issue Number 3, (2001)

Human Aldehyde Dehydrogenase Catalytic Activity and Structural Interactions with Coenzyme Analogs

www.adeninepress.com

Gonzalo Izaguirre[1] and Regina Pietruszko[1]
Samuel Cho and[2] Alexander D. MacKerell, Jr.[2*]

[1]Center of Alcohol Studies and Department of Molecular Biology and Biochemistry
Rutgers, the State University of New Jersey
Piscataway, NJ 08854-8001.

[2]Department of Pharmaceutical Sciences
School of Pharmacy
University of Maryland
Baltimore, MD 21201

Abstract

K_m and V_{max} values for 10 coenzyme analogs never previously studied with any aldehyde dehydrogenase and $NADP^+$ were compared with those for NAD^+ for three human aldehyde dehydrogenases (EC 1.2.1.3); the cytoplasmic E1 (the product of the *aldh1* gene), the mitochondrial E2 (the product of the *aldh2* gene) and the cytoplasmic E3 (the product of the *aldh9* gene) isozymes. Structural information on changes in coenzyme-protein interactions were obtained via molecular dynamics (MD) studies with the E2 isozyme and quantum mechanical (QM) calculations were used to study changes in charge distribution of the pyridine ring and relative free energies of solvation of the purine ring in the analogs. E1 showed the broadest substrate specificity and was the only isozyme subject to substrate inhibition, both of which are suggested to be due to the two coenzyme conformations observed previously in the sheep crystal structure. $NADP^+$ selectivity is indicated to be influenced by Glu195 in E1 and E2. Substitutions in the purine ring affected K_m but not V_{max}, with the changes in K_m being dominated by the hydrophobicity of the purine ring as indicted by the QM calculations. Substitutions in the pyridine ring sometimes rendered the coenzymes inactive, with no consistent pattern observed for the three coenzymes. Structural analysis of the coenzyme analog-E2 MD simulations revealed different structural perturbations of the surrounding active site, though interactions with Asn169 and Glu399 were preserved in all cases.

Introduction

Aldehyde dehydrogenase (EC 1.2.1.3) catalyzes dehydrogenation of a large variety of aldehydes in the presence of nicotinamide adenine dinucleotide (NAD^+) as the coenzyme. Evidence for 12 genes coding for aldehyde dehydrogenase in man has been reviewed (1). The genes coding for human aldehyde dehydrogenases of broad substrate specificity are: *aldh1*, *aldh2*, *aldh3*, *aldh9* and *aldh10*. While products of the *aldh1* gene (here called E1), *aldh2* gene (E2) and *aldh9* gene (E3) show strong preference for NAD^+ and are tetrameric enzymes, those of the *aldh3* and *aldh10* genes have dual coenzyme specificity and occur as a dimer and a polymer, respectively. The product of *aldh9* gene has also been described in the literature as aminobutyraldehyde, betaine aldehyde or trimethylaminobutyraldehyde dehydrogenase as it was at first believed to be a specific enzyme. Kinetic mechanisms for E1 (2) and E2 (3) have been determined. Both mechanisms are compulsory ordered with NAD binding before aldehyde. With E1, the rate limiting step is NADH dissociation while it is deacylation with E2. The kinetic mechanism of E3 has yet to be determined. Three-dimensional (3D) structures from X-ray crystallography for the gene products of *aldh1* (sheep liver), *aldh2* (bovine, human liver) *aldh3* (rat liver) and *aldh9* (cod liver) have been recently published (4-7).

Research efforts in recent years have concentrated on aldehyde dehydrogenase interactions with aldehyde substrates, which form covalent enzyme-acyl intermediates, rather than with coenzyme substrates. X-ray crystallography, however, has

*Correspondence to be addressed to:
Phone: 410-706-7442
Fax: 410-706-0346
E-mail: alex@outerbanks.umaryland.edu

demonstrated that the coenzyme-binding site of aldehyde dehydrogenases differs from that of other dehydrogenases and is composed of five β strands connected by four α-helices(5) instead of six β-strands common to NAD^+-dependent dehydrogenases (8,9). This difference has been confirmed by X-ray crystallography of the bovine mitochondrial enzyme, the product of *aldh2* gene (7), and of the cod liver cytoplasmic enzyme (4) product of *aldh9* gene. Differences in the coenzyme binding site of the three aldehyde dehydrogenases examined to date are evident by sequence and 3D structural comparisons but their significance cannot be interpreted without supporting kinetic data. However, specificity of human aldehyde dehydrogenases towards coenzyme analogs has never previously been investigated except for comparisons of the activity of NAD^+ vs. $NADP^+$. This lack of experimental kinetic data on coenzyme analogs motivated the present study.

It has long been recognized with dehydrogenases, in general, that major modifications in the purine moiety of the coenzyme are tolerated in retaining coenzyme functioning (10). Pyridine-modified analogs, however, are less tolerated and only a few of them are known to function as coenzymes. The specific binding of complex molecules such as NAD^+ or $NADP^+$ to dehydrogenases is mediated by selective interactions between different enzyme amino acid residues and different parts of the dinucleotide molecules. Both purine and pyridine analogs cannot function if they are not bound or poorly bound to the coenzyme binding site. If binding is too strong dissociation may be difficult and, thereby, coenzyme function could also be impaired. In addition, changes in the reduction potential of the nicotinamide moiety due to the chemical modification will impact coenzyme function. Thus, a combination of enzyme-coenzyme interactions and electronic properties of the nicotinamide contribute to the functionality of various coenzyme analogs.

Theoretical methods offer a powerful tool to investigate biological molecules, often allowing for an atomic detail interpretation of experimental data (11). For example, theoretical studies based on empirical force fields and molecular dynamics (MD) simulations allow for a full representation of the protein and the substrate and have been used to study protein conformation (12) and protein-substrate interactions (13), including the impact of pH on binding (14). Quantum mechanical (QM) approaches (15) typically cannot be used to study protein-ligand complexes, however, they can be used to investigate the electronic properties of individual organic molecules (16,17). In combination, application of MD and QM methods to protein-substrate interactions offers a powerful tool to help elucidate the structural determinants of experimentally observed kinetic properties. Indeed, the first computational study of an aldehyde dehydrogenase, the dimeric isozyme from the *aldh3* gene from rat, was recently published (18).

In this paper we present kinetic parameters for human liver homotetrameric E1, E2 and E3 isozymes obtained with coenzymes and coenzyme analogs. In addition, MD and QM based computational studies were performed on the studied coenzyme analogs, including interactions with the E2 isozyme. The kinetic parameters where then interpreted with respect to enzyme-coenzyme interactions, changes in electronic structure and changes in free energies of solvation obtained from the computational studies.

Materials and Methods

Experimental

Materials: Adult human autopsy livers were from National Disease Research Interchange (Philadelphia, PA). β-nicotinamide adenine dinucleotide (NAD^+) was from Boehringer-Mannheim (Indianapolis, IN). Propionaldehyde from Aldrich Chem Co. was redistilled before use. Betaine aldehyde, 3- acetylpyridine-AD^+, 3-pyridinealdehyde-AD+, nicotinic acid-AD^+, thionicotinamide-AD^+, N-1,N^6-ethenoadenine-D^+, N-hypoxanthine-D^+, N-guanine-D^+, acetylpyridine hypoxan-

thine-D^+, $NADP^+$, and α-NAD^+ were from Sigma-Aldrich (St. Louis, MO).

Purification of Enzymes: The E1 and E2 isozymes of human liver aldehyde dehydrogenase were purified from liver to homogeneity following the procedure of Hempel et al. (19). The purity was confirmed by SDS-PAGE electrophoresis and by isoelectric focusing. There was no cross contamination of E1 isozyme with the E2 isozyme and vice versa. Prior to use, E1 and E2 isozyme preparations were dialyzed vs. 25 mM sodium phosphate buffer, pH 6.0 to remove 2-mercaptoethanol and NAD^+ was used to stabilize the isozymes during storage. The E3 isozyme was purified as described by Kurys et al.(20); on SDS-PAGE it migrated as a single 54-kDa band. The E3 isozyme was stored at -10˚C in 20% v/v glycerol containing 0.1% v/v 2-mercaptoethanol, under nitrogen. Prior to use, aliquots of the enzyme preparation were loaded on a MonoP column from Pharmacia (Piscataway, NJ) using a Beckman FPLC system and washed with 10 mM sodium phosphate buffer, pH 6.8, containing 1 mM EDTA to remove glycerol and 2-mercaptoethanol. The enzyme was eluted with a gradient of sodium chloride which between 250 and 300 mM separates the E3 isozyme into two components (20). Only the major component of the E3 isozyme was used in these experiments.

Protein Determination: Protein concentration was determined employing the microbiuret method (21) using bovine serum albumin as standard.

Enzyme Activity Assays: To determine active enzyme concentration the enzyme activity was determined in 100 mM sodium phosphate buffer, pH 9.0 containing 1mM EDTA, 500 μM NAD^+ and 1mM propionaldehyde at 340 nm and 25ºC every day before start of experiments. In these conditions 1 mg of enzyme produces 0.6 μmol NADH/min/mg with both E1 and E3 isozymes: the E2 isozyme produces 1.6 mmol/min/mg. Kinetics with coenzyme analogs was also done at 340 nm, except for thionicotinamide-AD^+ which was monitored at 395 nm. A Gilford recording spectrophotometer with a circulating water bath and methacrylate 1 ml disposable cuvettes were used. Activities of the E1 and E2 isozymes were determined in 100 μM sodium phosphate buffer, pH 7.4, containing 500 μM propionaldehyde. With the E3 isozyme, kinetics were done in 100 mM sodium phosphate buffer, pH 9.0 containing 1 mM betaine aldehyde. Reactions were started by addition of enzyme. Duplicate or triplicate rate determinations were done at different concentrations of coenzyme analogs. The following extinction coefficients were used: 6.22 mM^{-1} cm^{-1} for NADH, NADPH, and for reduced N-1,N^6-ethenoadenine-D^+, N-hypoxanthine-D^+ and N-guanine-D^+ (22-25); 5.1 mM^{-1} cm^{-1} for reduced 3- acetylpyridine-AD^+ and 3-acetylpyridine hypoxanthine-D^+ (25,26); 6.0 mM^{-1} cm^{-1} for reduced 3-pyridinealdehyde-AD^+ (27); 4.6 mM^{-1} cm^{-1} for reduced nicotinic acid-AD^+ (28) and 5.6 mM^{-1} cm^{-1} for αNADH (29). An extinction coefficient of 11.9 mM^{-1} cm^{-1} at 395 nm was used for reduced thionicotinamide-AD^+ (30).

Kinetic constants were calculated by the Lineweaver-Burk (31) procedure employing the statistical method of Cleland (32). For ordered Bi-Bi kinetic mechanisms K_m and V_{max} for coenzymes (substrate A) represent complex mixtures of rate constants, dominated by terms associated with product formation and product release. Dividing V_{max} by K_m results in considerable simplification due to rate constant cancellation. The ratio V_{max}/K_m is equal to k_1, the ON-velocity constant for coenzyme binding (33).

Computational

Molecular Modeling and Dynamics Simulations: All modeling and simulations were performed using CHARMM(34,35) with the Merck Molecular Force Field (MMFF)(36). The crystal structure used for the tetrameric E2 isoenzyme with a single NAD^+ bound to each of the monomers is classified under the PDB code 1CW3(37). Due to the extensive size of ALDH, all calculations were performed *in*

vacuo on a truncated system that contained a single active site and the coenzyme or a coenzyme analog. The enzyme was truncated by deleting all residues without atoms within 18 Å of the NAD^+ from the first monomer. All remaining residues without atoms within 10 Å of the NAD^+ were selected to be a harmonically constrained buffer region when energy minimization and MD simulations were performed. Then the waters, the ions, and NAD^+ molecule were deleted, resulting in the desired truncated isoenzyme to be used with each of the coenzyme analogs. The terminal residues created by the truncation process were capped with acetyl groups so that energy calculations could be performed using MMFF.

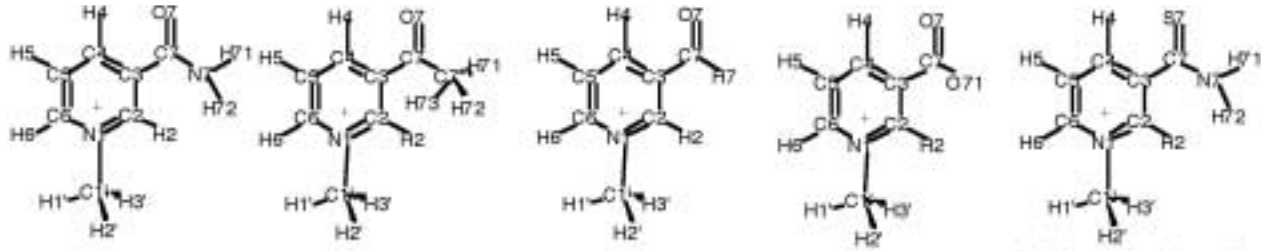

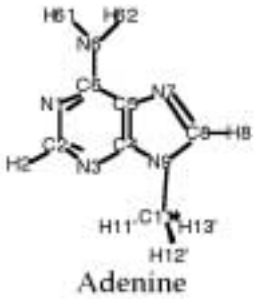

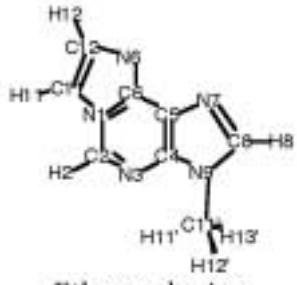

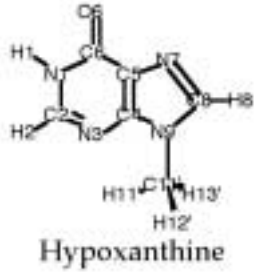

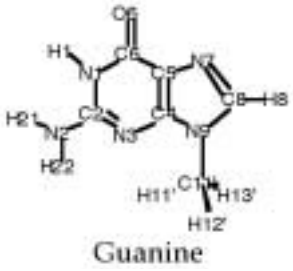

Figure 1: Chemical structures and nomenclature of pyridine and purine analog analogs used in the quantum mechanical studies.

The coenzyme analogs were constructed using SYBYL (Tripos Assoc. Inc.). With $NADP^+$ both the dianonic and monoanionic states of the phosphate moiety were studied. To place the analogs into the active site, all atoms in each of the analogs common to NAD^+ were assigned the NAD^+ cartesian coordinates. Then, the unique atoms were built based on the internal coordinates. The complexes were minimized using the Adopted Basis Newton-Raphson (ABNR) algorithm for 100 steps while harmonically constraining the entire structure with a force constant of 2.0 kcal/mol/Å^2. The structure was then further minimized, with the harmonically constrained buffer region subjected to a force constant of 2.0 kcal/mol/Å^2, for 500 steps of ABNR to allow the coenzyme to relax into the active site.

MD simulations were performed for 100 ps for each of the E2-coenzyme complexes using the minimized structures as a starting point. The simulations used the Leapfrog algorithm at 300 K with a step size of 0.002 ps. The SHAKE algorithm was employed to constrain all bonds involving hydrogen atoms(38). Nonbonded interactions were truncated at 12 Å using the force shift and switch methods to smooth the electrostatic and Lennard-Jones interactions, respectively, with the Lennard-Jones switching function turned on at 10 Å, the nonbond atom list maintained to 14 Å and updated heuristically. The buffer region residues were harmonically constrained with a force constant of 2.0 kcal/mol/Å^2. Coordinates were saved every 0.5 ps, of which the final 50 ps of the trajectories were used for analysis. Distances between the heavy atoms of the pyridine or adenine rings with the heavy atoms of the isoenzyme were calculated for each of the complexes during the course of the simulation to determine interactions that may have contributed to the measured kinetic parameters. The average distance between all pairs of heteroatoms with a cutoff distance of 4.0 Å during any point of the trajectory were considered, such that new interactions introduced during the course of the simulation would be identified. Of those identified, only those atom pairs with an average distance of less than 4.0 Å and involved in favorable hydrogen bond or electrostatic interactions where included in the final analysis. The average root mean square (RMS) differences for each of the coenzyme analogs was calculated by orienting the enzyme with respect to the constrained backbone region and comparing the positions of the conserved atoms between the crystal NAD^+ and the coenzyme analogs.

Quantum Mechanical Calculations: The Gaussian98 program(39) was used for all *ab intio* quantum mechanical calculations. The starting structures consisted of the coordinates for the pyridine or purine moiety generated using SYBYL, with the attached ribose sugar replaced with a methyl group. The model compounds are shown in Figure 1. The structures were optimized at the HF/6-31G* basis set to

default tolerances. The Mulliken and Natural Bond Orbital (NBO) methods (40) were applied to determine the charge distributions associated with each atom in the rings. Free energies of solvation of the purine analogs were obtained using the IPCM reaction field solvation model (41,42) assuming a dielectric constant of 78. Free energies were obtained as the difference between the gas phase and aqueous phase energies using the gas phase optimized structures for both calculations.

Results

Kinetic Constants for Coenzyme Analogs with the E1 Isozyme: K_m values and V_{max} of the E1 isozyme with the different coenzymes are presented in Table I.

Table I

Kinetic Constants of Human E1 Isozyme with βNAD⁺ and Analogs.

Analog	Km (±S.E.)	Vmax (±S.E.)	Vmax/Km x 1000	Analog Ratio(%)
βNAD⁺	4.7±1.3	0.2±0.02	49	100
βNADP⁺ [1]	7680±490	0.23±0.01	0.03	0.06
αNAD⁺ [2]	Inactive	Inactive	-	0
βNAD⁺-Substitutions in the Purine Ring:				
N-1,N⁶-Ethenoadenine-D⁺	11.3±2.6	0.28± 0.02	25	51
N-Hypoxanthine-D⁺	121±7.2	0.22±0.005	1.8	3.7
N-Guanine-D⁺	1390±180	0.20±0.02	0.15	0.3
βNAD⁺-Substitutions in the Pyridine Ring:				
3-Acetylpyridine-AD⁺	13.2±2.1	0.25±0.02	18.9	38.6
3-Pyridinealdehyde-AD⁺	504±5.7	0.24±0.01	0.48	1.0
3-Thionicotinamide-AD⁺ [3]	15.1±4.8	0.0102±0.002	0.0007	0.0015
3-Nicotinic Acid-AD⁺ [4]	Inactive	Inactive	-	0
βNAD⁺-Substitutions in the Purine and Pyridine Rings:				
3-Acetylpyridine-Hypoxanthine-D⁺ [5]	Inactive	Inactive	-	0

S.E = standard error of the Mean. K_m = μM; V_{max} = μmol/min/mg active enzyme protein; analog ratio = V_{max}/K_m analog/V_{max}/K_m βNAD⁺ x 100. [1] - substrate inhibition observed at concentrations above 10 mM; [2] tested at 0.1 - 2.0 mM, no inhibition observed at 250 μM vs. 300 μM βNAD⁺; [3] - substrate inhibition observed at concentrations above 15 μM (see Figure 2); [4] tested at 0.06 - 2.0 mM, no inhibition observed at 250 μM vs. 300 μM βNAD⁺. [5] - tested at 0.04 - 2.0 mM, no inhibition observed at 250 μM vs. 300 μM βNAD⁺.

Eight of the analogs were active, while the compounds, αNAD⁺, 3-nicotinic acid-AD⁺ and 3-acetylpyridine-hypoxanthine-D⁺ were inactive. For the active analogs the V_{max} values remained constant and appeared to be independent of coenzyme structure. The only exception was 3-thionicotinamide-AD⁺ with the V_{max} value considerably lower than that of other coenzymes. The K_m values, however, were sensitive to changes in the coenzyme structure, showing more than two orders of magnitude variability. These differences in K_m are reflected in the V_{max}/K_m ratios and in the analog ratios derived from these values. The coenzyme with the highest V_{max}/K_m ratio was NAD⁺ followed by N-1,N⁶-ethenoadenine-D⁺ and 3-acetylpyridine-AD⁺, N-hypoxanthine-D⁺, 3-pyridinealdehyde-AD⁺ and N-guanine-D⁺. βNADP⁺ at concentrations higher than 10 mM and 3-thionicotinamide-AD⁺ exhibited substrate inhibition of the E1 isozyme. The substrate concentration curve for 3-thionicotinamide-AD⁺ is shown in Figure 2. Pronounced substrate

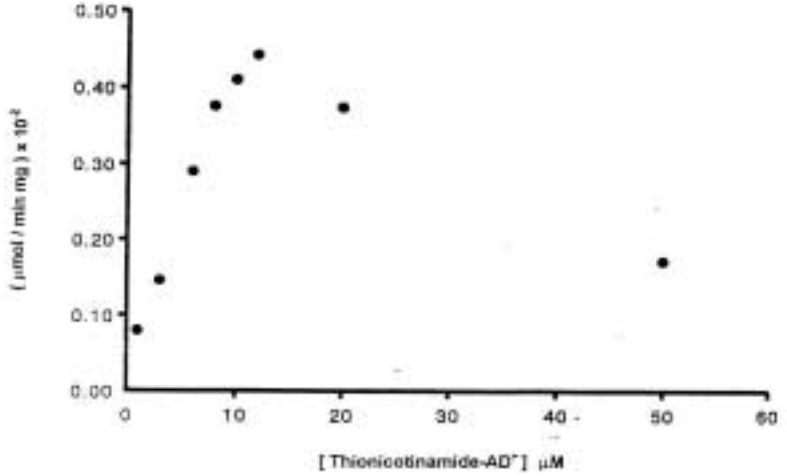

Figure 2: Substrate inhibition of human aldehyde dehydrogenase E1 by thionicotinamide-AD⁺. Reaction conditions as described in Materials and Methods.

inhibition occurs at 3-thionicotinamide-AD⁺ concentrations above ca. 12 mM. The three inactive coenzymes, αNAD⁺, 3-nicotinic acid-AD⁺ and 3-acetylpyridine-

hypoxanthine-D^+ were also tested as inhibitors of E1 activity. However, at the concentrations tested (see footnote of Table 1) no inhibition or activation of E1 activity was detected, indicating that binding to the enzyme did not occur at the tested concentrations.

Kinetic Constants for Coenzyme Analogs with the E2 Isozyme: The E2 isozyme was active with only seven coenzymes. The V_{max} values varied approximately 4 fold, with the highest velocity obtained with N-hypoxanthine-D^+, followed by N-1,N^6-ethenoadenine-D^+, βNAD$^+$, N-guanine-D^+, 3-acetylpyridine-AD^+ and 3-pyridinealdehyde-AD^+. As with the E1 isozyme, the greatest differences were observed in K_m values. Comparisons of V_{max}/K_m and analog ratios demonstrated that βNAD$^+$ and N-1,N^6-ethenoadenine-D^+ were almost indistinguishable. 3-Pyridinealdehyde-AD^+ had the next highest V_{max}/K_m ratio, due to its low K_m value, followed by 3-acetylpyridine-AD^+, N-hypoxanthine-D^+ and N-guanine-D^+. Four of the analogs, αNAD$^+$, 3- thionicotinamide-AD^+, 3-nicotinic acid-AD^+ and 3-acetylpyridine-hypoxanthine-D^+, were inactive at the concentrations tested (see footnote of Table 2). With the exception of 3-thionicotinamide-AD^+, they appeared

Table II

Kinetic Constants of Human E2 Isozyme with βNAD$^+$ and Analogs

Analog	Km (±S.E.)	Vmax (±S.E.)	Vmax/Km x 1000	Analog Ratio(%)
βNAD$^+$	94±8.4	0.46±0.01	4.9	100
βNADP$^+$	>10 000	ND	-	-
αNAD$^+$ [1]	Inactive	Inactive	-	0
βNAD$^+$-Substitutions in the Purine Ring:				
N-1,N^6-Ethenoadenine-D$^+$	96.0±7.3	0.47±0.01	4.9	100
N-Hypoxanthine-D$^+$	1360±140	0.50±0.02	0.37	7.6
N-Guanine-D$^+$	9680±2900	0.34±0.07	0.035	0.7
βNAD$^+$-Substitutions in the Pyridine Ring:				
3-Acetylpyridine-AD$^+$	620±98	0.27±0.02	0.44	9.0
3-Pyridinealdehyde-AD$^+$	33.8±3.9	0.10±0.002	3.0	61
3-Thionicotinamide-AD$^+$ [2]	Inactive	Inactive	-	0
3-Nicotinic Acid-AD$^+$ [3]	Inactive	Inactive	-	0
βNAD$^+$-Substitutions in the Purine and Pyridine Rings:				
3-Acetylpyridine-Hypoxanthine-D$^+$ [4]	Inactive	Inactive	-	0

S.E. = standard error of the Mean. K_m = μM; V_{max} = μmol/min/mg active enzyme protein; analog ratio = V_{max}/K_m analog/V_{max}/K_m βNAD$^+$ x 100. [1] - No activity at 0.1-2 mM αNAD$^+$, no inhibition or activation when 250 μM αNAD$^+$ was used vs. 280 μM βNAD$^+$; [2] - no activity at 10-100 μM; strong inhibition vs. βNAD$^+$ (see Figure 3); [3] - no activity at 0.1-2 mM; no inhibition or activation at 280 μM vs. 250 μM βNADP$^+$. [4] - No activity at 0.1-2 mM, no inhibition or activation at 200 μM vs. 250 μM βNAD$^+$.

not to bind to the enzyme in that they had no effect on enzyme activity with other coenzymes. 3-Thionicotinamide-AD^+ produced strong inhibition of NAD^+ activity, showing that it was binding to the enzyme (Figure 3). Only slope effects were

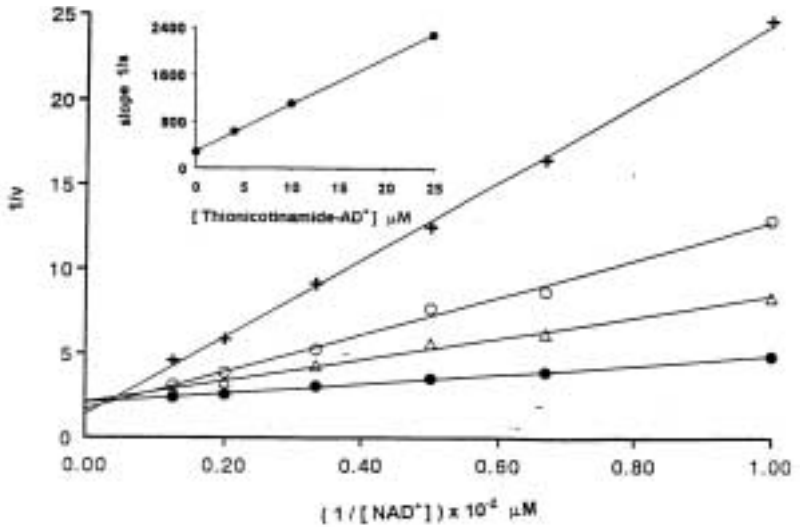

Figure 3: Inhibition of human aldehyde dehydrogenase E2 by thionicotinamide-AD^+. The reactions were done at constant (500 mM) propionaldehyde concentrations, at varied NAD+ and different fixed thionicotinamide-AD^+ concentrations. V = μmol NADH formed/min/mg of E2 isozyme; J - J thionicotinamide-AD^+ = 0; C - C thionicotinamide-AD^+ = 4 μM; E - E thionicotinamide-AD^+ = 10 μM; + - + thionicotinamide-AD^+ = 25 μM. Reaction conditions as described in Materials and Methods. Inset shows replot of slopes vs. thionicotinamide-AD^+ concentrations. The calculated dissociation constant was 3.7 μM.

observed (Fig. 3), showing that it was a competitive inhibitor versus varied NAD^+. The K_i value for 3-thionicotinamide-AD^+ was obtained from data in Figure 3 and found to be 3.7 μM, indicating it to bind tightly to the enzyme.

Kinetic Constants for Coenzyme Analogs with the E3 Isozyme: Due to the limited amount of enzyme available, the coenzyme specificity was tested with betaine aldehyde as the substrate at pH 9.0, where the catalytic activity is higher than at pH 7.4 used for the E1 and E2 isozymes. Only six of the coenzymes tested were active with the E3 isozyme (Table 3). The highest V_{max} was observed with N-guanine-

Table III

Kinetic Constants of Human E3 Isozyme with βNAD⁺ and Analogs.

Analog	Km (±S.E.)	Vmax (±S.E.)	Vmax/Km x 1000	Analog Ratio(%)
βNAD⁺	23.4±2.4	8.7±0.3	372	100
βNADP⁺ [1]	Inactive	Inactive	-	0
αNAD⁺ [2]	Inactive	Inactive	-	0
βNAD⁺-Substitutions in the Purine Ring:				
N-1,N⁶-Ethenoadenine-D⁺	35.8±3.0	20.0±0.47	559	150
N-Hypoxanthine-D⁺	172±12	16.8±0.47	98	26.3
N-Guanine-D⁺	944±140	31.4±2.0	33	9
βNAD⁺-Substitutions in the the Pyridine Ring:				
3-Acetylpyridine-AD⁺	102±7.8	12.4 ±0.3	122	33
3-Pyridinealdehyde-AD⁺ [3]	Inactive	Inactive	-	0
3-Thionicotinamide-AD⁺	14.6±0.74	9.95±0.15	682	183
3-Nicotinic Acid-AD⁺ [4]	Inactive	Inactive	-	0
βNAD⁺-Substitutions in the Purine and Pyridine Rings:				
3-Acetylpyridine-Hypoxanthine-D⁺ [5]	Inactive	Inactive	-	0

S.E. = standard error of the Mean. K_m = μM; V_{max} = μmol/min/mg active enzyme protein; adjusted to known velocities; analog ratio = V_{max}/K_m analog/ V_{max}/K_m βNAD⁺ x 100. [1] - No activity at 0.1-10 mM, at 1.2 mM no effect on enzyme activity at 300 μM βNAD⁺; [2] - no activity at 0.2-2 mM, no effect at 700 μM on enzyme activity at 280 μM βNAD⁺; [3] - no activity at 0.1-1 mM, strong inhibition of activity with N-hypoxanthine-D⁺ (see Figure 4); [4] - no activity at 0.2-2 mM; no effect at 660 μM on enzyme activity at 280 μM βNAD⁺; [5] - no activity at 1 mM and 2 mM, no effect at 740 μM on enzyme activity at 290 μM βNAD⁺.

D^+ and the lowest with βNAD^+, showing a 3 fold difference. Variability was also observed in the K_m values. From V_{max}/K_m and analog ratios it can be seen that 3-thionicotinamide-AD^+ had the highest ratio followed by N-1,N^6-ethenoadenine-D^+, NAD^+, 3-acetylpyridine-AD^+, N-hypoxanthine-D^+ and N-guanine-D^+. 3-Pyridinealdehyde-AD^+ was inactive but inhibited the enzyme when tested versus N-hypoxanthine-D^+ (Figure 4). The K_i value for 3-pyridinealdehyde-AD^+ calcu-

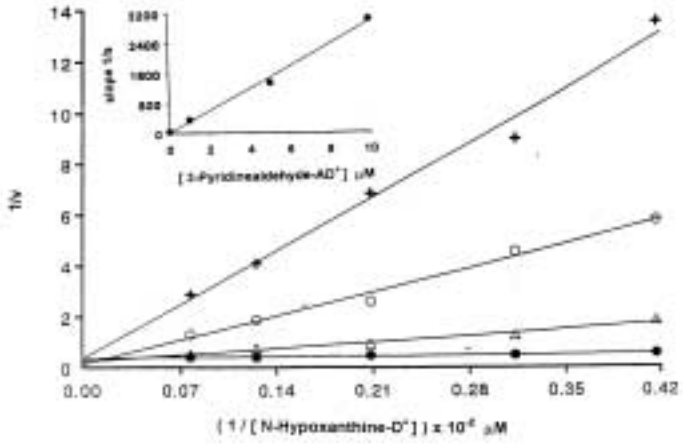

Figure 4: Inhibition of human aldehyde dehydrogenase E3 by pyridinealdehyde-AD^+. The reactions were done at constant (1 mM) betaine aldehyde concentrations at varied N-hypoxanthine- D^+, and different fixed pyridinealdehyde-AD^+ concentrations. V = μmol N-hypoxanthine-DH formed/min/mg of E3 isozyme; J - J pyridinealdehyde-AD+ = 0; C - C pyridinealdehyde-AD^+ = 1 μM; E - E pyridinealdehyde-AD^+ = 5 μM; + - + pyridinealdehyde-AD^+ = 10 μM. Reaction conditions as described in Materials and Methods. Inset: replot of slopes vs. pyridinealdehyde-AD^+ concentrations. The calculated dissociation constant was 0.062 μM.

lated from slope replots in the competitive pattern observed (Figure 4) was found to be very small, 0.062 μM, indicating strong binding to enzyme. No activity or binding of the other four coenzymes listed as inactive in Table 3 was detected at the concentrations tested.

Comparison of E1, E2 and E3 Isozyme's Coenzyme Specificity. The E1 isozyme exhibited substrate inhibition with coenzymes (Table 1 and Figure 1); no substrate inhibition with any of the coenzymes tested was observed with E2 and E3 during this investigation. The maximal velocity of the E2 and E3 isozymes (Tables 2 and 3) responded to changes in coenzyme structure; V_{max} of the E1 isozyme remained constant with the exception of 3-thionicotinamide-AD^+ (Table 1). In general, coenzyme analogs substituted in the adenine ring behaved similarly with all three isozymes, in that their effectiveness as substrates decreased from 1,N^6-etheno-NAD^+ to N-guanine- D^+ and was largely the result of increasing K_m values, indicating an important role of the purine ring in influencing the V_{max}/K_m ratio. There

were differences in the three enzymes with respect to coenzymes substituted in the pyridine ring. 3-Acetylpyridine-AD^+ appeared to be a reasonably good substrate for the E1 and E3 isozymes, but was somewhat worse for the E2 isozyme. The E3 isozyme was inactive with 3-pyridinealdehyde-AD^+, although that analog was active, but a poor substrate for E1 and E2. Notably, binding of pyridinealdehyde-AD^+ to the E3 isozyme could be easily demonstrated (Figure 4), with a K_I value of 0.062 μM. On the other hand, 3-thionicotinamide-AD^+ had low activity with the E1 isozyme (Table 1), was inactive, but readily bound with the E2 isozyme (Figure 3), while with the E3 isozyme it functioned as a good substrate, being a better substrate than NAD^+ (Table 3). The E1 and E2 isozymes were active with $NADP^+$; with E1 the K_m value was less than 10 mM; the K_m value for the E2 isozyme was not determined, but the enzyme was active with $NADP^+$ at a 10 mM concentration. At 10 mM $NADP^+$ the E3 isozyme was inactive.

MD simulaions of NAD^+ and the coenzyme analogs with the E2 isozyme: To better interpret the kinetic data MD simulations of the coenzymes with the E2 isozyme were undertaken. E2 was selected as it is the only isozyme of the three studied for which a structure of the human enzyme is available. Results from the simulations were analyzed with respect to overall changes in the position of the coenzyme and the protein and select moieties as based on RMS differences with respect to the crystal structures. RMS differences were also determined for the protein and for the catalytically essential amino acids, Cys302 (43,44) and Glu268 (45,46). In addition, analysis of specific interactions between the nicotinamide ring and the enzyme was performed. Concerning the protein, the RMS differences were generally in the range of 1 to 1.4 Å, indicating that the protein structure was maintained during the simulations (Table 4). The only exception was with nicotinic acid-AD^+, where a significantly larger difference of 1.77 Å occurred. For Cys302 structural

Table IV

Average RMS difference between the crystal structure and the protein during the MD simulations

Analog	Enzyme[1]	Cys 302	Glu 268[2]
NAD^+	1.09±0.03	1.70±0.18	1.87±0.09
$NADP^+$ (dianionic)	1.13±0.02	1.81±0.32	1.95±0.08
$NADP^+$ (monoanionic)	1.24±0.03	1.67±0.24	1.95±0.08
ßNAD+-Substitutions in the Purine Ring:			
N-1, N^6-Ethenoadenine-D^+	1.36±0.03	1.68±0.25	1.83±0.08
N-Hypoxanthine-D^+	1.18±0.02	1.89±0.18	1.93±0.10
N-Guanine-D^+	1.23±0.03	1.91±0.27	1.88±0.09
ßNAD+-Substitutions in the the Pyridine Ring:			
3-Acetylpyridine-AD^+	1.13±0.02	1.82±0.20	1.88±0.09
3-Pyridinealdehyde-AD^+	1.13±0.02	1.10±0.14	1.91±0.08
Thionicotinamide-AD^+	1.19±0.03	1.92±0.20	1.90±0.09
Nicotinic Acid-AD^+	1.77±0.04	1.08±0.18	1.99±0.09
ßNAD+-Substitutions in the Purine and Pyridine Rings:			
3-Acetylpyridine-Hypoxanthine-D^+	1.11±0.02	1.20±0.17	1.91±0.09

RMS differences in Å. RMS differences for the protein only include those residues in the truncated system that were not subjected to harmonic constraints.

Table V

Average RMS difference between the crystal structure and the coenzymes during the MD simulations

Analog	Coenzyme[2]	PyridineRing[2]	Purine Ring[2]
NAD^+	1.13±0.08	0.55±0.12	0.97±0.29
$NADP^+$ (dianonic)	1.17±0.08	0.51±0.10	0.55±0.14
$NADP^+$ (monoanionic)	2.13±0.12	0.54±0.11	2.80±0.24
ßNAD+-Substitutions in the Purine Ring:			
N-1, N^6-Ethenoadenine-D^+	1.15±0.04	0.61±0.13	0.53±0.15
N-Hypoxanthine-D^+	1.54±0.06	1.04±0.10	0.62±0.20
N-Guanine-D^+	1.11±0.06	0.57±0.13	0.52±0.13
ßNAD+-Substitutions in the the Pyridine Ring:			
3-Acetylpyridine-AD^+	1.15±0.08	0.64±0.11	1.04±0.28
3-Pyridinealdehyde-AD^+	1.20±0.06	0.92±0.10	0.86±0.19
Thionicotinamide-AD^+	1.18±0.08	0.76±0.11	1.08±0.18
Nicotinic Acid-AD^+	1.23±0.10	1.35±0.12	0.72±0.21
ßNAD+-Substitutions in the Purine and Pyridine Rings:			
3-Acetylpyridine-Hypoxanthine-D^+	1.30±0.07	1.45±0.10	0.70±0.20

RMS differences in Å.

differences were generally in the range of 1.7 to 2.0 Å, though smaller changes were observed for 3-pyridinealdehyde-AD$^+$, nicotinic acid-AD$^+$ and 3-acetylpyridine-hypoxanthine-D$^+$. With Glu268 the structural differences were all in the vicinity of 1.9 Å. RMS differences involving the coenzyme are reported in Table 5. Structural changes of the entire coenzyme were generally in the range of 1.1 to 1.2 Å, with larger changes occurring in monoanionic NADP$^+$, 3-acetylpyridine-hypoxanthine-D$^+$ and N-hypoxanthine-D$^+$. With the pyridine ring, the structural changes were generally below 1 Å, except with N-hypoxanthine-D$^+$, 3-nicotinic acid-AD$^+$ and 3-acetylpyridine-hypoxanthine-D$^+$. Differences of approximately 1 Å or less were observed for all the purine rings with the exception of monoanionic NADP$^+$ where a value of 2.8 Å was obtained.

Specific interactions involving the pyridine moiety of the coenzyme with the enzyme are presented in Figures 5 through 8. Figure 5 presents interactions

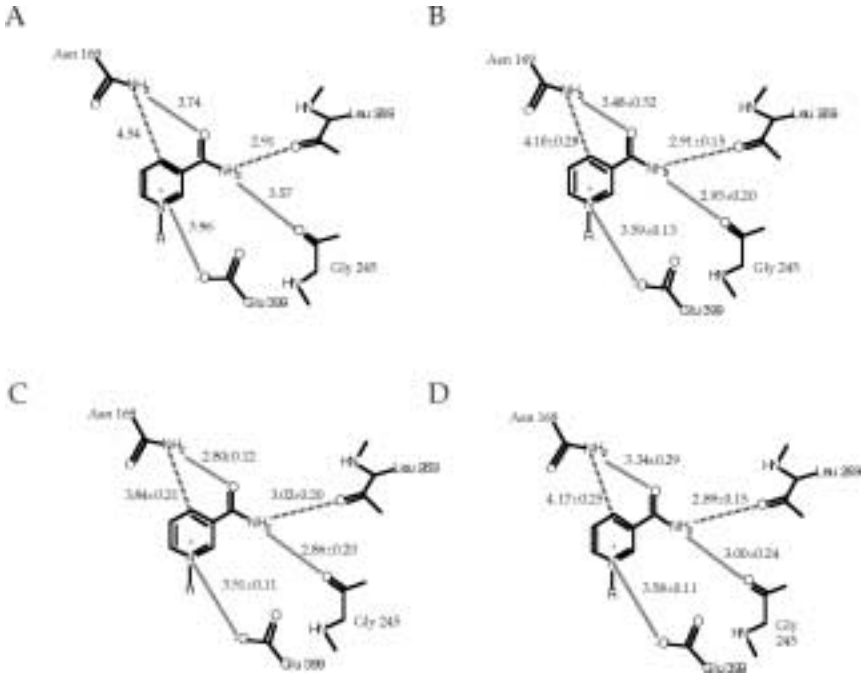

Figure 5: Diagram of nicotinamide binding to the E2 active site for the A) E2-NAD$^+$ crystal structure, B) the E2-NAD$^+$ MD averages C) the E2-NADP$^+$(monoanionic) MD averages and D) the E2-NADP$^+$ (dianionic) MD averages. For the MD structures the average distances and standard deviations are reported.

observed in the experimental crystal structure (37) along with those for the βNAD$^+$ and βNADP$^+$ simulations. Comparison of Fig. 5a and 5b shows the interactions observed in the crystal to generally be maintained in the MD simulation. With both βNADP$^+$ species (Fig. 5c and 5d) these interactions are also maintained. For the analogs involving alterations of the purine ring, the pattern of interactions is well maintained, except with N-hypoxanthine-D$^+$, where the interactions between Gly245 or Leu269 and the amide nitrogen are lost and replaced by an interaction with the peptide carbonyl of the catalytically essential Cys302 (Fig. 6). More vari-

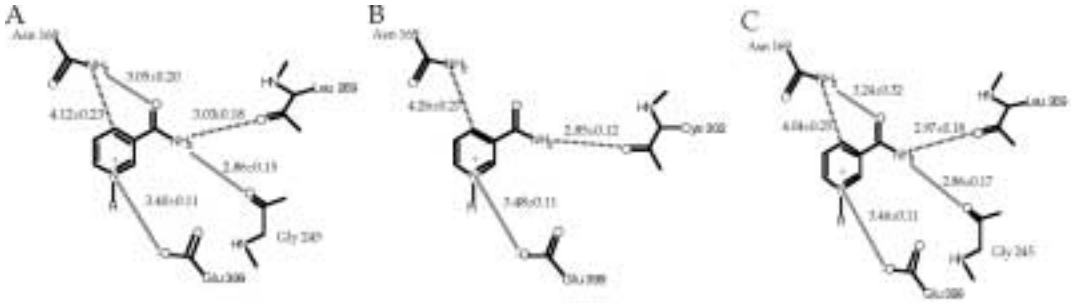

Figure 6: Diagram of nicotinamide binding to the E2 active site for the purine modified analogs: A) N-1, N^6-Ethenoadenine-D$^+$, B) N-Hypoxanthine-D$^+$, and C) N-Guanine-D$^+$. Average distances and standard deviations from the MD simulations are reported.

ation in the interactions with the pyridine moiety occurred when that moiety itself was modified, as expected (Fig. 7). Modification of the amide moiety lead to differences in the interactions with the enzyme (compare Figs. 5 and 7), while interactions involving Asn169 and Glu399 with the pyridine ring itself were maintained

with all 4 analogs. With the 3-thionicotinamide-AD^+ analog a hydrogen bond between Cys302 and the thioamide occurs. Modification of both the pyridine and purine moieties in 3-acetylpyridine-hypoxanthine-D^+ (Fig. 8) leads to an interaction pattern almost identical to that of 3-acetylpyridine-D^+.

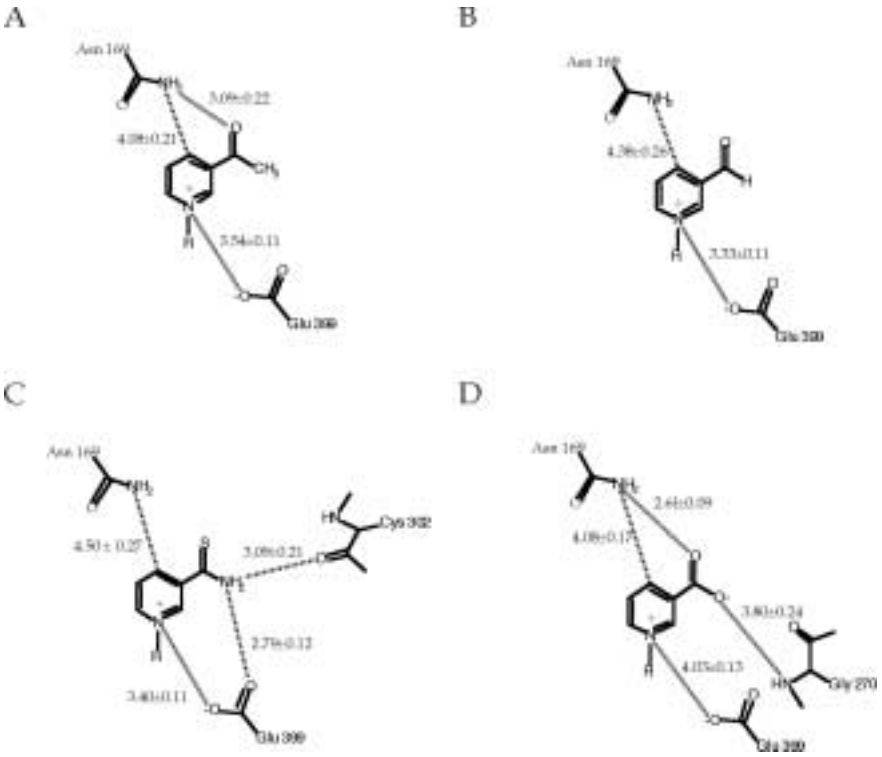

Figure 7: Diagram of the pyridine analogs binding to the E2 active site for the pyridine modified analogs: A) 3-acetylpyridine-AD^+, B) 3-Pyridinealdehyde-AD^+, C) 3-thionicotinamide-AD^+, and D) 3-nicotinic acid-AD^+. Average distances and standard deviations from the MD simulations are reported.

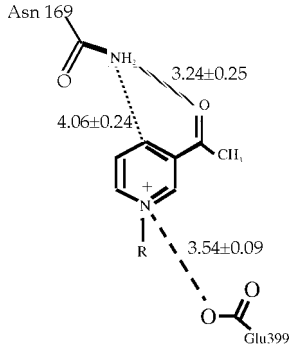

Figure 8: Diagram of the pyridine analog binding to the E2 active site for 3-acetylpyridine-hypoxanthine-D^+. Average distances and standard deviations from the MD simulations are reported.

Pyridine Charge Distributions and Purine Solvation Energies via Quantum Mechanical Calculations: Alteration of the reduction potential associated with changes in the chemical composition of the pyridine moiety may also contribute to changes in chemical reactivity, with effects on V_{max} expected to dominate. In E1 and E2, where NADH dissociation and deacylation are the rate limiting steps, respectively, changes in the kinetic mechanism associated with the coenzyme analogs could lead to hydride transfer becoming the rate-determining step. Such a switch in the rate-determining step has been observed in E2 mutants (47). Rigorous calculation of the reduction potential would require explicit treatment of hydride transfer (48), a procedure that is very computationally intensive. However, analysis of differences in charge distribution in the nicotinamide C4 atom, to which hydride transfer occurs, may be assumed to give a first order approximation of pos-

Table VI
Partial atomic charges of the pyridine moieties based on quantum mechanical calculations

Nicotinamide			3-Acetylpyridine			3-Pyridinealdehyde			3-Thionicotinamide			Nicotinic Acid		
Atom	Mull.	NBO	Atom	Mull.	NBO	Atom	Mull.	NBO	Atom	Mull.	NBO	Atom	Mull.	NBO
N1	-0.60	-0.38	N1	-0.61	-0.38	N1	-0.63	-0.38	N1	-0.60	-0.38	N1	-0.59	-0.39
C2	0.18	0.15	C2	0.18	0.16	C2	0.18	0.17	C2	0.17	0.14	C2	0.17	0.16
H2	0.30	0.26	H2	0.30	0.26	H2	0.30	0.26	H2	0.30	0.26	H2	0.31	0.28
C3	-0.22	-0.20	C3	-0.21	-0.20	C3	-0.21	-0.22	C3	-0.12	-0.15	C3	-0.24	-0.19
C4	**-0.05**	**-0.02**	**C4**	**-0.05**	**-0.02**	**C4**	**-0.05**	**-0.02**	**C4**	**-0.06**	**-0.03**	**C4**	**-0.09**	**-0.06**
H4	0.33	0.29	H4	0.33	0.29	H4	0.33	0.29	H4	0.32	0.29	H4	0.30	0.28
C5	-0.28	-0.28	C5	-0.28	-0.28	C5	-0.28	-0.28	C5	-0.28	-0.28	C5	-0.28	-0.28
H5	0.30	0.28	H5	0.30	0.28	H5	0.30	0.28	H5	0.30	0.28	H5	0.25	0.26
C6	0.17	0.16	C6	0.18	0.17	C6	0.18	0.16	C6	0.17	0.16	C6	0.13	0.09
H6	0.30	0.26	H6	0.30	0.26	H6	0.30	0.26	H6	0.30	0.26	H6	0.25	0.24
C1'	-0.33	-0.40	C1'	-0.33	-0.40	C1'	-0.33	-0.40	C1'	-0.33	-0.40	C1'	-0.32	-0.40
H1'	0.26	0.26	H1'	0.24	0.25	H1'	0.25	0.25	H1'	0.24	0.25	H1'	0.22	0.24
H2'	0.24	0.25	H2'	0.25	0.25	H2'	0.26	0.26	H2'	0.26	0.26	H2'	0.22	0.24
H3'	0.24	0.25	H3'	0.25	0.25	H3'	0.24	0.25	H3'	0.24	0.25	H3'	0.23	0.24
C7	0.79	0.83	C7	0.58	0.67	C7	0.36	0.50	C7	0.19	0.13	C7	0.84	0.98
O7	-0.54	-0.65	O7	-0.48	-0.58	O7	-0.43	-0.55	S7	-0.13	-0.09	O7	-0.69	-0.83
N7	-0.92	-0.92	C7	-0.60	-0.74	H7	0.21	0.17	N7	-0.83	-0.85	O71	-0.71	-0.85
H71	0.40	0.42	H71	0.26	0.28				H71	0.44	0.45			
H72	0.43	0.45	H72	0.20	0.24				H72	0.41	0.42			
			H73	0.20	0.24									

Charges in electron units.

sible changes in reduction potential. Compounds designed to model the pyridine chemical modifications (see Fig. 1) were subjected to *ab initio* energy minimization following which the charge distributions were determined based on the Mulliken and Natural Bond Orbital methods (40). Presented in Table 6 are the partial atomic charges, with the values for the C4 atom shown in bold. For nicotinamide, 3-acetylpyridine, and 3-pyridinealdehyde the charges at the C4 position are identical, indicating no major change in the reduction potential. The C4 charge decreases from -0.05 in nicotinamide, based on the Mulliken analysis, to -0.06 in 3-thionicotinamide and -0.09 in nicotinic acid, suggesting that the reduction potential is more unfavorable with respect to hydride transfer. The trends from the Mulliken and NBO analysis were similar, indicating that the differences observed in the calculations are reliable.

The adenine moiety of NAD^+ is known to bind to a hydrophobic pocket in dehydrogenases. Accordingly, solvation of the purine ring could significantly impact binding to that site. Quantum calculations using a reaction field model (41,42) were therefore performed to obtain estimates of the free energies of solvation of the four purine analogs included in the study (see Fig. 1). Table 7 presents the calculated absolute free energies of solvation for the four purines. Of these, the least favorably solvated is the adenine moiety, followed by ethenoadenine, though the difference is only 0.4 kcal/mol. Both hypoxanthine and guanine are significantly more favorably solvated, with guanine being the most favorably solvated. While the present calculations exclude energetic contributions associated with geometry and vibrational contributions, those terms are expected to be small and similar based on the cyclic nature of the studied compounds. In addition, differences in free energies of solvation are expected to be more reliable than the absolute values (49).

Table VII
Free energies of solvation of purine analogs based on Quantum Mechanical reaction field calculations

Analog	Gas phase[1]	Aqueous Phase[1]	F.E. solvation[2]
adenine	-503.55344	-503.5840079	-19.18
ethenoadenine	-579.25997	-579.2912002	-19.60
hypoxanthine	-523.38266	-523.4180968	-22.25
guanine	-578.42749	-578.4664386	-24.44

1) Energies in hartrees.
2) Energies kcal/mol.

Discussion

To understand the effect of chemical alteration of the coenzyme structure on the activity of human aldehyde dehydrogenase a combined experimental and computational study has been undertaken. Experiments measured the K_m and V_{max} values for the coenzyme analogs studied in the E1, E2 and E3 isozymes. In cases where the analog was apparently not a substrate, experiments were performed to determine if the analogs were inhibitors, including inhibition kinetic analysis for two analogs (Fig. 3 and 4), with those analogs shown to be competitive with respect to NAD^+ and N-hypoxanthine-D^+, respectively. To facilitate interpretation of the kinetic data MD simulations were undertaken to determine how the different analogs interact with the E2 isozyme. The calculations were designed to investigate structural perturbation in the coenzyme analogs and regions of the protein adjacent to the analogs, including the catalytic residues Cys302 and Glu268. Due to the large number of analogs, the calculations were performed *in vacuo* on a truncated model of the enzyme that included only one active site and only on the E2-NAD^+(or analog) binary complex. Accordingly, results from the present MD calculations on the coenzyme analogs may only be interpreted in terms of local structural perturbations with respect to the control calculations on the enzyme-NAD^+ complex. The reliability and reproducibility of the MD results is verified by the reproduction of the crystal interaction pattern in both the NAD^+ and $NADP^+$ MD simulations (Fig. 5) as well as by the similarity of the pyridine-enzyme interactions in the 3-acetylpyridine-AD^+ (Fig. 7a) and 3-acetylpyridine-hypoxanthine-D^+ (Fig.

8) MD simulations. In addition, QM calculations were performed to determine changes in charge distribution of the pyridine moieties and relative solvation free energies of the purine moieties studied. The following discussion combines the experimental results with those from the computations to present a picture of the influence of coenzyme structure on catalytic activity.

The results obtained with human aldehyde dehydrogenases and listed in Tables 1, 2 and 3 show that all three enzymes behave in a similar way with the analogs modified at the purine ring, as shown by comparison of the V_{max}/K_m and analog ratios. Following NAD^+ N-1,N^6-ethenoadenine-D^+ is the best substrate while N-guanine-D^+ is the worst. In E1 and E2 (Tables 1 and 2) the K_m for N-1,N^6- ethenoadenine-D^+ increased relative to the K_m of NAD^+ and V_{max} was unaffected while in E3 (Table 3) only a slight increase in K_m occurred and V_{max} increased by more than 2-fold, making this compound a better substrate then NAD^+. This increase in V_{max} also occurred in the other two purine analogs with E3 while the K_m values increased significantly over NAD^+. MD simulations of the purine modified analogs show the overall structural changes to be small (Table 5) including in the vicinity of the nicotinamide moiety (Fig. 6). The largest changes occur in the N-hypoxanthine-D^+ analog, which includes the loss of hydrogen bonds between the nicotinamide ring and Leu269 and Gly245 and formation of a new hydrogen bond with Cys302 (Fig 6B). However, since the experimental V_{max} values for the N-hypoxanthine-D^+ analog were similar to or elevated over that of NAD^+ it may be assumed that the structural changes do not significantly effect the catalytic activity, though they may impact binding.

Changes in K_m for the three purine analogs may be related to changes in solvation of the purine moiety. This is consistent with the hydrophobic nature of the binding pocket and lack of hydrogen bonding between adenine and the enzyme (37). Since binding is an equilibrium between the unbound coenzyme in solution and bound to the enzyme, the more favorably solvated an analog is, the more it favors the equilibrium in solution (50) and presumably leads to a decrease in the On-velocity constant for coenzyme binding with the enzyme (see V_{max}/K_m ratios in Table 1, 2 and 3). Results presented in Table 7 show guanine to be the most favorably solvated purine followed by hypoxanthine with adenine and N-1,N^6-ethenoadenine being the least favorably solvated. Note that the 0.4 kcal/mol difference in solvation of adenine and N-1,N^6-ethenoadenine is probably not significant based on limitations in the applied reaction field model (49). The ordering of the free energies of solvation in Table 7 corresponds well with the K_m values for all three isozymes. This result, combined with the minimal structural changes observed in the MD simulations, indicates that solvation effects significantly influence the V_{max}/K_m ratio of the coenzyme. Furthermore, it is interesting that the increased size of the N-1,N^6-ethenoadenine analog does not adversely impact binding. Analysis of the E2-NAD^+ crystal structure shows the N6 amino group of adenine, which corresponds to the region of the purine ring modified in N-1,N^6-ethenoadenine (Fig. 1), to protrude out towards solvent. Analysis of the final structure from the MD simulation showed this portion of the N-1,N^6-ethenoadenine moiety to, indeed, protrude from the enzyme, thereby avoiding steric overlap that could hinder binding.

In the present study major differences were observed between the three enzymes as a result of substitutions at position 3 of the nicotinamide (Tables 1, 2 and 3). The greatest differences were seen with 3-thionicotinamide-AD^+: it was inactive with the E2 isozyme, was a poor substrate for the E1 isozyme but was an excellent substrate for the E3 isozyme. With the E1 isozyme, where thionicotinamide-AD^+ acted as a substrate, no major change in K_m value as compared to the K_m for NAD^+ was observed; the only difference was the decrease in V_{max} (only approximately 4% of the velocity with NAD^+). With the E3 isozyme both K_m and V_{max} values were similar to that with NAD^+ (Table 3). Analysis of the MD simulation results shows the change of the nicotinamide amide oxygen to a sulfur to be well tolerat-

ed by the enzyme, as evidenced by RMS differences similar to those for NAD^+ (Tables 4 and 5). This is consistent with this analog being a competitive inhibitor of E2 activity vs. varied NAD^+. Furthermore, the calculated dissociation constant (3.7 μM; see legend to Figure 3), indicates that thionicotinamide-AD^+ binds well to the E2 isozyme. However, in E2 changes in hydrogen bonding occur (Fig. 7c), with the backbone carbonyl of Cys302 now hydrogen bonding to the thioamide. This change of Cys302 may lead to this analog being inactive with E2; the maintenance of activity in E1 and E3 suggest that the disruption of the active site seen in E2 is not occurring. With respect to the reduction potential, a small decrease in the C4 charge occurs in 3-thionicotinamide-AD^+, which may lower V_{max}. This is consistent with the kinetic data for E1; however in E3, the V_{max} is comparable to that of NAD^+. Interestingly, in E3, NAD^+ has the lowest V_{max} of the active coenzymes indicating that the mentioned change in the reduction potential of 3-thionicotinamide-AD^+ may be influencing V_{max}. Clearly, in E3 the enzyme is impacting the reduction potential of the nicotinamide in a manner that differs from E1 and E2. This, as of yet not understood contribution, could lead to the higher V_{max} for 3-thionicotinamide-AD^+ with E3.

Differences in coenzyme function were also seen with 3-pyridinealdehyde-AD^+, which functioned as a substrate with the E1 and E2 isozymes but was inactive with the E3 isozyme. In the case of the E1 isozyme the K_m value was increased approximately 100 fold relative to that of NAD^+ with V_{max} remaining unchanged (Table 1). With the E2 isozyme both the K_m and V_{max} values were lower than those of NAD^+ (Table 2). RMS differences from the MD simulations on the E2 isozyme showed structural changes in 3-pyridinealdehyde-AD^+ to be similar to those in NAD^+, with the only difference being a smaller structural change in Cys302 (Table 4) and a larger structural change for the coenzyme pyridine moiety (Table 5). Analysis of the interactions involving the pyridine moiety show the loss of hydrogen bonds with protein residues that interact with the amide moiety of NAD^+ (compare Fig. 5b and Fig. 7b). This loss of interactions, while the C4 charges are identical to those of NAD^+ (Table 6), is suggested to lead to the decreased V_{max} with the E2 isozyme, possibly due to poor positioning of the nicotinamide during catalysis. The inactivity of this analog with E3 will require additional computational studies, though the mechanism causing E3 to have larger V_{max} values with all the analogs as compared to NAD^+ (Table 3) may be responsible. Such altered interactions involving the nicotinamide may also be responsible for this compound being a potent inhibitor of E3 with a K_i of 0.062 μM (see legend of Fig. 4).

Unlike the above mentioned pyridine analogs, 3-acetylpyridine-AD^+ was a reasonable substrate for the E1 and E3 isozymes (Table 1 and 3); however, it was ten fold less effective than NAD^+ for E2 as seen by comparison of the V_{max}/K_m values and analog ratios. Structural information from the MD simulations show 3-acetylpyridine to be well behaved with respect to RMS differences (Tables 4 and 5), though substitution of the methyl group for the amino group on the nicotinamide moiety of NAD^+ led to a loss of some interactions that occur in NAD^+ (compare Fig. 5b and Fig. 7c). This loss of interactions is suggested to contribute to the increased K_m and decreased V_{max} values with the E2 isozyme as compared to NAD^+.

$NADP^+$, tested at a 10 mM concentration, was inactive with the E3 isozyme, was active with the E2 isozyme, but its K_m value was not determined and was active with E1, having a K_m of 7.7 mM. The K_m value for $NADP^+$ for the E2 isozyme equivalent from rat liver mitochondria has been determined to be 67.2 mM (51); the K_m for the human E2 isozyme is probably similar. The fact that no activity was observed with the E3 isozyme at 10 mM $NADP^+$ suggests that its K_m for $NADP^+$ is even larger than that of the E2 isozyme. Based on the MD simulations, $NADP^+$ interacts with E2 in a manner identical to NAD^+ for the nicotinamide (see Tables 4 and 5, Fig. 5), though significant differences occur in the adenine with the monoanionic species of $NADP^+$. These results are consistent with $NADP^+$ also being a sub-

strate, with the large RMS difference with the monoanionic species possibly contributing to the increased K_m. To understand in detail the possible impact of the additional phosphate in $NADP^+$ on interactions with the enzyme, nonbond interactions between the AO2' atom of NAD^+ or the AO2' phosphate oxygens of $NADP^+$ with protein nitrogen or oxygen atoms where investigated, with the results shown in Table 8. In both the NAD^+ crystal and MD simulation structures there is a direct

Table VIII

Interaction distances between the AO2' atom of NAD^+ or the AO2' phosphate oxygens of $NADP^+$ and protein heteroatoms in E2

Coenzyme atom	Protein atom	Distance, Å
NAD^+ Crystal		
AO2'	LYS192-NZ	2.85
AO2'	GLU195-OE1	5.44
AO2'	GLU195-OE2	2.43
AO2'	GLY225-N	3.95
NAD^+ Final MD structure		
AO2'	LYS192-NZ	5.55
AO2'	GLU195-OE1	5.18
AO2'	GLU195-OE2	2.89
AO2'	GLY225-N	3.48
$NADP^+$(dianionic) Final MD structure		
AO2'	LYS192-NZ	5.15
AO2'	GLU195-OE2	4.10
O71	ILE386-N	2.55
O71	LYS192-O	5.65
O71	VAL193-N	3.70
O72	PRO167-N	3.68
O72	VAL193-O	3.99
O72	ALA194-N	2.57
O73	LYS192-NZ	2.41
O73	VAL193-N	3.36
O73	VAL193-O	3.24
O73	ALA194-N	3.57
O73	GLU195-OE2	3.98
$NADP^+$ (monoanionic) Final MD structure		
O71	LYS192-NZ	2.96
O71	VAL193-O	3.93
O72	GLU195-N	4.17
O72	GLU195-OE2	3.56
O73	LYS192-NZ	2.78
O73	GLU195-N	3.31
O73	GLU195-OE1	3.18
O73	GLU195-OE2	2.56
O73	GLY225-N	3.79

Interactions between the listed coenzyme oxygens and protein heteroatoms (N and O) less than 4 Å in the NAD crystal structure and the final time frames from the NAD^+ and $NADP^+$ - E2 MD simulations. The AO2' to GLU195-OE2 $NADP^+$ interaction was identified by searching for GLU195 to phosphate oxygen interactions less than 4.5 Å.

interaction of the AO2' atom with Glu195. This residue is conserved in E1 and E2 and was suggested to stabilize coenzyme binding in class 3 aldehyde dehydrogenase (*aldh3* gene product) based on the crystal structure (52). More recently this suggestion was verified based on mutational analysis, though the results suggested that alternate residues may also contribute to coenzyme specificity (53). In the two E2-$NADP^+$ complexes there are a significant number of interactions between the phosphate and the protein, including the positively charged sidechain of Lys192. Interactions of Glu195 and AO2' are still present with dianionic $NADP^+$ but the distance has increased from 2.9 Å in the NAD^+ MD structure to 4.1 Å and a O73 to Glu195 OE2 interaction of 4.0 Å is present. With monoanionic $NADP^+$ several interactions occur between the phosphate oxygens and Glu195. These results suggest that the coenzyme binding site, in which the AO2' atom is sequestered from the surface in E2, can accommodate the phosphate in $NADP^+$, allowing it to be a substrate for E1 and E2. However, the presence of Glu195 may be considered to have unfavorable interactions with the $NADP^+$ AO2' phosphate and, therefore, is predicted to contribute to the coenzyme specificity for NAD^+. This is also consistent with studies on *Vibrio harveyi* aldehyde dehydrogenase, where mutation of a threonine to a glutamate at the position corresponding to Glu195 led to a change in coenzyme specificity from $NADP^+$ to NAD^+ (54). Accordingly, mutation of Glu195 in E2 is predicted to perturb the coenzyme specificity in favor of $NADP^+$. It should be noted that this residue is not conserved in E3, where it is replaced by a proline (55). This change and the lack of activity of E3 with $NADP^+$ at the tested concentrations indicate that the mechanism of coenzyme selectivity of that isozyme may differ from E1 and E2.

Several coenzyme analogs tested during this investigation were found to be inac-

tive with all three isozymes. These included αNAD$^+$, 3-nicotinic acid-AD$^+$ and the dual substituted 3-acetylpyridine-hypoxanthine-D$^+$ analogs (Tables 1, 2 and 3). All three analogs were shown not to act as inhibitors with all three isozymes and, therefore, may be assumed to not bind or bind poorly to the enzyme. In αNAD$^+$ the different chirality about the C1' atom of the sugar bound to the nicotinamide will disallow the nicotinamide to access its binding pocket when the remainder of the coenzyme is bound to the enzyme (or vice versa), thereby disallowing binding. With 3-nicotinic acid-AD$^+$ the negative charge leads to significant structural distortion of the enzyme (Table 4) and of the pyridine moiety of the coenzyme (Table 5) as well as significantly different interactions with the acid group versus the normal amide (Fig. 7d). The need for these structural changes to occur is suggested to be responsible for that analog not binding to the enzyme. Moreover, based on the changes in the C4 atom charge (Table 6), if this analog did bind it is doubtful that it would undergo hydride transfer. The dual modifications in the 3-acetylpyridine-hypoxanthine-D$^+$ analog each individually lead to increases in K_m for all three isozymes (Tables 1, 2 and 3). The combination of these increases is suggested to lead to its inability to bind.

Only the E1 isozyme exhibited substrate inhibition with coenzymes. This substrate inhibition was observable with 3-thionicotinamide-AD$^+$ (Fig. 2) but was also noticeable with NADP$^+$. Inhibition with NAD$^+$ was never observed; other coenzyme analogs were not investigated sufficiently with the E1 isozyme to see if at some high concentrations they may inhibit. Substrate inhibition with coenzymes is rare in dehydrogenases, although an incidence of this has been reported (56). Recently, the structure of the sheep *aldh1* gene product has been obtained via X-ray crystallography (6). In those studies the NAD$^+$ was observed to bind in two conformers. Only one major coenzyme binding conformation has been observed in the E2 crystal structure (37), in the gene product of bovine *aldh2* (7), which bears strong structural resemblance to E2, and in the gene product of cod liver *aldh9* (4), which resembles the human E3 isozyme. No substrate inhibition with any coenzymes or analogs was observed with the E2 or E3 isozymes during this investigation. These results suggest that the coenzyme conformers in E1 observed via crystallography may be responsible for the observed substrate inhibition. Interestingly, the major conformer was previously assigned to be "catalytically nonproductive" while the minor conformer was indicated to be similar to the conformation seen in E2 (6). Thus, the presence of two coenzyme conformers in the crystal structure of E1 appears to be related to the presence of substrate inhibition in that system. The presence of two coenzyme conformations also indicates the E1 binding site to be more promiscuous than in E2 or E3. This may be responsible for the E1 substrate specificity being the broadest of the three isozymes studied, and may contribute to the disparity between the activities of thionicotinamide-AD$^+$ and pyridinealdehyde-AD$^+$ analog discussed in the preceding paragraph.

It is possible that thionicotinamide-AD$^+$ and pyridinealdehyde-AD$^+$ (Figs. 3 and 4) are in fact substrates with extremely low velocities, which are not easily detectable in spectrophotometric measurements, such that the inhibition constants determined during this investigation are actually K_m values. The possibility that these analogs can act as substrates is supported by the QM calculations showing the C4 charges to be similar to those of nicotinamide (Table 6). In recent work we demonstrated that some aldehyde inhibitors of aldehyde dehydrogenase were substrates with low velocities (57,58) suggesting that similar mechanism could also operate with coenzyme analogs. It is clear, however, from our experiments that thionicotinamide and pyridinealdehyde coenzyme analogs distinguish the coenzyme binding sites of E1, E2 and E3 aldehyde dehydrogenases. Differences in E1 may be related to two NAD$^+$ conformers observed in the crystal structure, however, the available X-ray structures of the E2 and analogous E3 isozyme do not allow for the different kinetic properties to be understood.

In the kinetic mechanism of the E1 isozyme, coenzyme dissociation is the rate limiting step (2) versus deacylation for the E2 isozyme (3); the rate-limiting step for the E3 is unknown though V_{max} differs widely with aldehyde substrates of different structure. However, analysis of the V_{max} values for the different coenzyme analogs with E1 show them all to be nearly identical, with the exception of 3-thionicotinamide-AD^+, where a significant decrease occurs. Though speculative, this similarity suggests that in E1 a conformational change in the enzyme following dissociation of the acid product may be responsible for the coenzyme dissociation rate, such that changes in coenzyme structure have little impact on V_{max}. With 3-thionicotinamide-AD^+ and E1 the significant decrease in V_{max} suggests that the rate-limiting step in the kinetic mechanism has changed. The variation in V_{max} in E2 is also small, consistent with coenzyme dissociation occurring prior to the rate-limiting deacylation step. The largest exception occurs with 3-pyridinealdehyde-AD^+, where the approximately 4-fold decrease suggests a change in the rate-limiting step. Detailed kinetic studies on the rate-limiting steps are required to clarify these points.

Details of the catalytic mechanism of aldehyde dehydrogenase are still under investigation. Mechanisms have been proposed for E2 (7) and for the *aldh3* gene product (59). In the former mechanism Cys302 and Glu268 are indicated to be catalytic residues, while in the latter it is suggested that Cys302 (Cys243 in *aldh3*), Asn169 (Asn114 in *aldh3*) and Glu399 (Glu333 in *aldh3*) are catalytic residues. In both models Cys302 is proposed to be the enzyme nucleophile involved in the covalent intermediate. Asn169 is conserved in all ALDH's (60). In E2 this residue is suggested to stabilize the oxyanion during formation of the covalent intermediate, while in the *aldh3* mechanism it is proposed to act as a general acid, donating a proton to the substrate carbonyl oxygen upon formation of the covalent intermediate and during the deacylation step. To support this latter proposition the authors discuss a 3D structure that includes benzaldehyde modeled into the active site (52) and data that mutation of Asn169 to Asp in *aldh3* decreases activity to 0.6 % that of native enzyme (59). The general base in the E2 mechanism it suggested to be Glu268, consistent with chemical modification(45,46) and mutagenesis data (61). In the *aldh3* proposed model Glu399 (Glu333 in *aldh3*) is suggested to act as a general base to extract a proton from an active site water allowing the water to accept the proton from Cys302 (Cys243 in *aldh3*) during formation of the covalent intermediate and facilitating the nucleophilicity of the water during deacylation. Indeed, via mutagensis it has been shown that changing Glu399 leads to a change in the rate limiting step (47,62), and this residue has been proposed to position the nicotinamide of NAD^+ in E2 (7). In all the coenzyme analogs subject to MD simulations in the present study, as well as in the crystallographic structure of E2, Asn169 and Glu399 interact with the nicotinamide or related moiety. While the presented calculations were not designed to study the role of individual residues in catalysis, they do support important roles for Asn169 and Glu399 in stabilizing the location of the nicotinamide moiety of NAD^+; however, they do not exclude the roles suggested for *aldh3*. Moreover, differences in the kinetic data on the coenzyme analogs for the highly homologous E1, E2 and E3 isozymes are consistent with different catalytic mechanisms. It is to be expected that even larger differences may exist between E2 and the *aldh3* gene product.

Conclusion

Presented is a combined experimental and theoretical structure-function study on the relationship of coenzyme structure to kinetic properties in three aldehyde dehydrogenases. While the computational studies were only on a single active site, versus the full E2 tetramer, and *in vacuo* they do facilitate interpretation of the present as well as previously published experimental data. Results presented are consistent with those obtained with other dehydrogenases in that substitutions in the adenine ring generally do not interfere with coenzyme function in that only K_m val-

ues but not maximal velocities are effected. The significant contribution of hydrophobicity in the adenine binding pocket is emphasized by the correlation between K_m and computed free energies of solvation. Based on the MD simulation the adenine binding pocket is able to accommodate the sterically large N-1,N^6-ethenoadenine purine analog without perturbing interactions between the coenzyme and the protein. The aldehyde dehydrogenase isozymes studied in the present work are known to be specific for NAD^+ over $NADP^+$. This was confirmed in the present study and, based on the known X-ray structures and the present calculations, Glu195 is indicated to contribute to coenzyme specificity in E1 and E2. However, Glu195 is replaced by Pro in the E3 isozyme, which did not have activity with $NADP^+$, suggesting that the mechanism of coenzyme specificity may differ in this isozyme, consistent with the present kinetic data.

Like other dehydrogenases, aldehyde dehydrogenase is more sensitive to substitutions in the pyridine ring which in some cases (thionicotinamide-AD^+, pyridinealdehyde-AD^+ and nicotinic acid-AD^+) interfere with coenzyme function. The broader substrate specificity of E1 and the presence of substrate inhibition in that isozyme only is suggested to be due to additional promiscuity of its coenzyme binding site as compared to E2 and E3. This is suggested to be associated with the two coenzyme-binding modes observed in the sheep liver *aldh1* structure (6). In E2, analysis of MD simulations indicate that different structural modifications of the nicotinamide moiety will impact enzyme-coenzyme interactions in different ways depending on the type of modification. Also, QM calculations indicate that changes in the charge distribution, that could impact the reduction potential, must be consider during a structure-function analysis. Based on the MD simulations Asn169 and Glu399 are observed to interact with the pyridine moiety in all the analogs. This supports important roles for these residues in catalysis, though the exact nature of those roles was not addressed in this work.

The present kinetic data may also be exploited in the design of assays to identify specific aldhehyde dehydrogenases in biological fluids. Thionicotinamide-AD^+, which is inactive with the E2 isozyme could be useful for assay of the E1 and E3 isozymes present in a mixture. Alternatively, pyridinealdehyde-AD^+ could serve for the assay of the E1 and E2 isozymes, excluding E3. Such approaches could also exploit differences in aldehyde specifities although differences in maximal velocities would have to be taken into account.

Abbreviations - Nicotinamide adenine dinucleotide, NAD^+; nicotinamide adenine dinucleotide phosphate, $NADP^+$; nicotinamide 1,N6-ethenoadenine dinucleotide, N-1,N6-ethenoadenine-D^+; nicotinamide hypoxanthine dinucleotide, N-hypoxanthine-D^+; nicotinamide guanine dinucleotide, N-guanine-D^+; 3-acetylpyridine adenine dinucleotide, 3-acetylpyridine-AD^+; 3-pyridinealdehyde adenine dinucleotide, 3-pyridinealdehyde-AD^+; 3-thionicotinamide adenine dinucleotide, 3-thionicotinamide-AD^+; 3-nicotinic acid adenine dinucleotide, 3-nicotinic acid-AD^+; 3-acetylpyridine hypoxanthine dinucleotide, 3-acetylpyridine-hypoxanthine-D^+.

Acknowledgements

Financial support of USPHS NIAAA Grant 1R02 AA00186 to R.P. and NIH GM51505 to A.D.M, Jr. is acknowledged.

References and Footnotes

1. A. Yoshida, A. Rzhetsky, L. C. Hsu, C. Chang *Eur. J. Biochem. 251*, 549-557 (1998)
2. R. C. Vallari, R. Pietruszko *Arch Biochem Biophys. 212*, 9-19 (1981)
3. R. S. Sidhu, A. H. Blair *J. Biol. Chem. 250*, 7894-7904 (1975)
4. K. Johansson, M. El-Ahmad, S. Ramaswamy, L. Hjelmqvist, H. Jornvall, H. Eklund *Protein Sci. 7*, 2106-17. (1998)

5. Z. J. Liu, Y. J. Sun, J. Rose, Y. J. Chung, C. D. Hsiao, W. R. Chang, I. Kuo, J. Perozich, R. Lindahl, J. Hempel, W. B. C. *Nat Struct Biol. 4*, 317-26. (1997)
6. S. A. Moore, H. M. Baker, T. J. Blythe, K. E. Kitson, T. M. Kitson, B. E. N. *Structure. 6*, 1541-51. (1998)
7. C. G. Steinmetz, P. Xie, H. Weiner, T. D. Hurley *Structure. 5*, 701-11. (1997)
8. M. G. Rossman, A. Lilias, C.-I. Branden, L. J. Banaszek *Evolutionary and structural relationships among dehydrogenases*; Boyer, P. D., Ed., 1970; Vol. 11, pp 63-102.
9. M. G. Rossman, D. Moras, K. W. Olsen *Nature 250*, 194-199 (1974)
10. B. M. Anderson, N. O. Kaplan *Model studies and biological activity of analogs*; Dolphin, D., Poulson, R. and Abramovic, O., Ed.; John Wiley and Sons Inc.: New York, 1987, pp 569-611.
11. O. M. Becker, J. MacKerell, A.D., B. Roux, M. Watanabe *Computational Biochemistry and Biophysics*; Marcel-Dekker, Inc.: New York, 2001, pp 512.
12. L. S. Caves, J. D. Evanseck, M. Karplus *Protein Sci. 7*, 649-666 (1998)
13. D. Yin, X. Yang, Y. Hu, K. Kuczera, R. L. Schowen, R. T. Borchardt, T. C. Squier *Biochemistry 39*, 9811-9818 (2000)
14. A. D. MacKerell, Jr., M. S. Sommer, M. Karplus *J. Mol. Biol 247*, 774-807 (1995)
15. W. J. Hehre, L. Radom, P. v. R. Schleyer, J. A. Pople *Ab Initio Molecular Orbital Theory*; John Wiley & Sons: New York, 1986.
16. P. N. V. Pavandumar, P. Seetharamulu, S. Yao, J. D. Saxe, D. G. Reddy, F. H. Hausheer *J. Comp. Chem. 20*, 365-382 (1999)
17. K. B. Wiberg, C. M. Hadad, C. M. Breneman, K. E. Laidig, M. A. Murcko, T. J. LePage *Science 252*, 1266-1271 (1991)
18. T. Wymore, H. B. Nicholas, J. Hempel *Chem. Biol. Interact. 130-132*, 201-207 (2001)
19. J. D. Hempel, D. M. Reed, R. Pietruszko *Alcohol Clin Exp Res. 6*, 417-25. (1982)
20. G. Kurys, W. Ambroziak, R. Pietruszko *J Biol Chem. 264*, 4715-21. (1989)
21. J. Goa *Scand. J. Clin. Lab. Invest. 5*, 218-222 (1953)
22. J. R. Barrio, J. A. Secrist, III., N. J. Leonard *Proc. Ntl. Acad. Sci. USA 69*, 2039-2042 (1972)
23. B. L. Horecker, A. Kornberg *J. Biol. Chem. 175*, 385-390 (1948)
24. A. M. Stein *FEBS Letters 19*, 270-272 (1971)
25. J. van Eys, M. M. Ciotti, N. O. Kaplan *J. Biol. Chem. 231*, 571-582 (1958)
26. N. O. Kaplan, M. M. Ciotti *J. Biol. Chem. 221*, 823-832 (1956)
27. N. O. Kaplan, M. M. Ciotti, F. E. Stolzenbach *J. Biol. Chem. 221*, 833-844 (1956)
28. M. Lamborg, F. E. Stolzenbach, N. O. Kaplan *J. Biol. Chem. 231*, 685-694 (1958)
29. G. Pfleiderer, C. Woenckhaus, N. Nelbock-Hochsteter *Ann. Chem. 690*, 170-176 (1965)
30. A. M. Stein, J. K. Lee, C. D. Anderson, B. M. Anderson *Biochemistry 2*, 1015-1017 (1963)
31. H. Lineweaver, D. Burk *J. Am. Chem. Soc. 56*, 658-667 (1934)
32. W. W. Cleland *Meth. Enzymol. 63*, 103-138 (1979)
33. I. H. Segel *Enzyme Kinetics. Behavior and Analysis of Rapid Equilibrium and Steady-State Enzyme Systems*; John Wiley & Sons: New York, 1975.
34. B. R. Brooks, R. E. Bruccoleri, B. D. Olafson, D. J. States, S. Swaminathan, M. Karplus *J. Comput. Chem. 4*, 187-217 (1983)
35. A. D. MacKerell, Jr., B. Brooks, C. L. Brooks, III, L. Nilsson, B. Roux, Y. Won, M. Karplus *CHARMM: The Energy Function and Its Paramerization with an Overview of the Program*; P.v.R. Schleyer, N. L. A., T. Clark, J. Gasteiger, P.A. Kollman, H.F. Schaefer III, P.R. Schreiner, Ed.; John Wiley & Sons: Chichester, 1998; Vol. 1, pp 271-277.
36. T. A. Halgren *J. Comput. Chem. 17*, 490-519 (1996)
37. L. Ni, J. Zhou, T. D. Hurley, H. Weiner *Protein Sci. 8*, 2784-90. (1999)
38. J. P. Ryckaert, G. Ciccotti, H. J. C. Berendsen *J. Comp. Phys. 23*, 327-341 (1977)
39. M. J. Frisch, G. W. Trucks, H. B. Schlegel, G. E. Scuseria, M. A. Robb, J. R. Cheeseman, V. G. Zakrzewski, J. A. Montgomery, Jr., R. E. Stratmann, J. C. Burant, S. Dapprich, J. M. Millam, A. D. Daniels, K. N. Kudin, M. C. Strain, O. Farkas, J. Tomasi, V. Barone, M. Cossi, R. Cammi, B. Mennucci, C. Pomelli, C. Adamo, S. Clifford, J. Ochterski, G. A. Petersson, P. Y. Ayala, Q. Cui, K. Morokuma, D. K. Malick, A. D. Rabuck, K. Raghavachari, J. B. Foresman, J. Cioslowski, J. V. Ortiz, A. G. Baboul, B. B. Stefanov, G. Liu, A. Liashenko, P. Piskorz, I. Komaromi, R. Gomperts, R. L. Martin, D. J. Fox, T. Keith, M. A. Al-Laham, C. Y. Peng, A. Nanayakkara, C. Gonzalez, M. Challacombe, P. M. W. Gill, B. Johnson, W. Chen, M. W. Wong, J. L. Andres, C. Gonzalez, M. Head-Gordon, E. S. Replogle, J. A. Pople *Gaussian 98*; Gaussian, Inc.: Pittsburgh, PA, 1998.
40. J. P. Foster, F. Weinhold *J. Am. Chem. Soc. 102*, 7211-7218 (1980)
41. V. Barone, M. Cossi, J. Tomasi *J. Comp. Chem. 19*, 404-417 (1998)
42. M. Cossi, V. Barone, R. Camni, J. Tomasi *Chem. Phys. Let. 255*, 327-335 (1996)
43. J. D. Hempel, R. Pietruszko *J Biol Chem. 256*, 10889-10896 (1981)
44. J. D. Hempel, R. Pietruszko, P. Fietzek, H. Jornvall *Biochemistry. 21*, 6834-6838 (1982)
45. A. D. MacKerell, Jr., R. S. MacWright, R. Pietruszko *Biochemistry. 25*, 5182-9. (1986)
46. D. P. Abriola, R. Fields, S. Stein, A. D. MacKerell, Jr., R. Pietruszko *Biochemistry. 26*, 5679-84. (1987)
47. S. Sheikh, L. Ni, T. D. Hurley, H. Weiner *J Biol Chem. 272*, 18817-22. (1997)
48. L. L. Ho, A. D. MacKerell, Jr., P. A. Bash *J. Phys. Chem. 100*, 2588-2596 (1996)

49. I.-J. Chen, A. D. MacKerell, Jr. *Theoretical Chemistry Accounts 103*, 483-494 (1999)
50. S. Lieske, B. Yang, M. E. Eldefrawi, A. D. MacKerell Jr., J. Wright *J. Med. Chem. 41*, 864-867 (1998)
51. P. C. Shah, S. C. Turan, R. Pietruszko *Alcohol. 8*, 25-30. (1991)
52. Z. J. Liu, J. Hempel, J. Sun, J. Rose, D. Hsiao, W. R. Chang, Y. J. Chung, I. Kuo, R. Lindahl, W. B. C. *Adv Exp Med Biol. 414*, 1-7 (1997)
53. J. Perozich, I. Kuo, B. C. Wang, J. S. Boesch, R. Lindahl, J. Hempel *Eur. J. Biochem. 267*, 6197-6203 (2000)
54. L. Zhang, B. Ahvazi, R. Szittner, A. Vrielink, E. Meighen *Biochemistry 38*, 11440-11447 (1999)
55. G. Kurys, P. C. Shah, A. Kikonygo, D. Reed, W. Ambroziak, R. Pietruszko *Eur J Biochem. 218*, 311-320. (1993)
56. S. Zepeda, O. Monasterio, T. Ureta *Biochem. J. 266*, 637-644 (1990)
57. A. Kikonyogo, D. P. Abriola, M. Dryjanski, R. Pietruszko *Eur J Biochem. 262*, 704-12. (1999)
58. G. Izaguirre, A. Kikonyogo, R. Pietruszko *Comp Biochem Physiol B Biochem Mol Biol. 119*, 747-54. (1998)
59. J. Hempel, J. Perozich, T. Chapman, J. Rose, J. S. Boesch, Z.-J. Liu, R. Lindahl, B.-C. Wang *Adv. Exper. Med. Biol. 463*, 53-59 (1999)
60. A. Perczel, Ö. Farkas, I. G. Csizmadia *J. Am. Chem. Soc. 117*, 1653-1654 (1995)
61. X. Wang, H. Weiner *Biochemistry. 34*, 237-43. (1995)
62. L. Ni, S. Sheikh, H. Weiner *J Biol Chem. 272*, 18823-6. (1997)

Date Received: August 14, 2001

Communicated by the Editor Ramaswamy H. Sarma